Transverse Scattering Matrix Formulation for a Class of Waveguide Eigenvalue Problems

Zhewang Ma, Eikichi Yamashita, *Fellow, IEEE,* and Shanjia Xu, *Senior Member, IEEE*

Abstract— **Based on the mode-matching procedure, a unified transverse scattering matrix formulation is presented for the characterization of a class of waveguide eigenvalue problems, which include not only closed but also open structures. As examples, calculations are carried out on the dispersion characteristics of ridged waveguides and its variations, nonradiative dielectric (NRD) waveguides, groove guides, microstrip lines, finlines, and coplanar waveguides. Comparisons with published data are made, which verify the versatility and accuracy of this method. Besides its generality, this approach is also superior to some other techniques in simplicity and numerical efficiency.**

I. Introduction

THE eigenvalue problem is one of the most fundamental problems in electromagnetic theory and engineering, and a variety of techniques have been developed for the characterization of various kinds of waveguiding structures in the past years [1]–[3]. Usually a different technique is employed for a different kind of transmission line in view of its simplicity, accuracy, and numerical efficiency, etc.

Microwave and millimeter-wave systems are being developed towards higher component densities and increasing complexity that may consist of various kinds of waveguiding structures. As a result, attention has been directed in recent years to generalized approaches that can treat a variety of transmission lines with complicated configurations. Thus, in developing a new technique the "generalization" has become another challenging factor to be considered in addition to its accuracy and numerical efficiency.

In this paper, based on the mode-matching procedure, the eigenvalue problems of a class of waveguiding structures are solved by combining the generalized scattering matrix technique with the transverse resonance method. The mode-matching and the transverse resonance method have been shown to be very versatile and effective in solving electromagnetic problems [1]–[3]. However, our theory in this paper features in the following characteristics:

1) With the generalized scattering matrix formulation of cascaded discontinuities in the transverse plane, the requirement of a proper choice of the expansion modal terms in the mode-matching method can be readily satisfied, and the solutions of eigenvalues converge quickly and correctly.

2) With the proper choice of the reference plane where the transverse resonance condition is applied, the size of the final eigenvalue matrix can be the smallest. Moreover, the eigenvalue matrix possesses the diagonal dominant property with the diagonal matrix elements of order 1, so that its determinant is neither too large nor too small. This fact greatly eases the numerical root searching process for the eigenvalue equation.

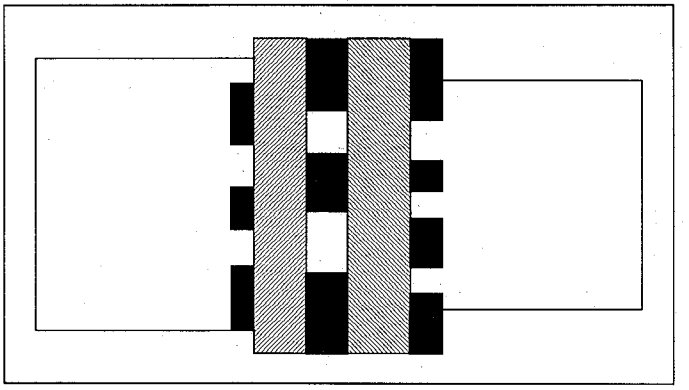

Fig. 1. Generalized waveguiding structure.

3) Open structures, such as the nonradiative dielectric (NRD) waveguide [4] and the groove guide [5], [6], etc., can be treated directly as special cases of our theory without any preassumptions. The two open ends in the NRD waveguide and the groove guide extend to infinity, and they may constitute an obstacle in applying the finite element method (FEM), the finite difference method (FDM), and the conventionally used transverse resonance process [7]. To overcome it, usually an assumption had to be made that perfect conductor planes were placed on the two sides of the guide which were far away from the dielectric strip or the groove [7]. In our approach, however, as is shown in Section III, such an assumption is not needed and the two open ends just simplify the final eigenvalue equation.

4) The formulation is quite general, and a wide variety of waveguiding structures can be handled with efficiency. Besides its versatility and flexibility, our theory, as discussed in detail in Section III, also overcomes some of the shortcomings of the previous techniques used in treating those waveguiding structures given in Section III.

Typical examples analyzed in this paper include ridged waveguides and its variations, NRD waveguides, groove guides, and planar transmission lines, and numerical results are compared with those of other authors.

II. Formulation

Figure 1 shows a generalized waveguiding structure. It consists of an arbitrary number of metallic strips deposited on various dielectric substrate interfaces. In general, the fields in the dielectric slab-loaded, ridged waveguide may be expressed

0018–9480/93$03.00 © 1993 IEEE

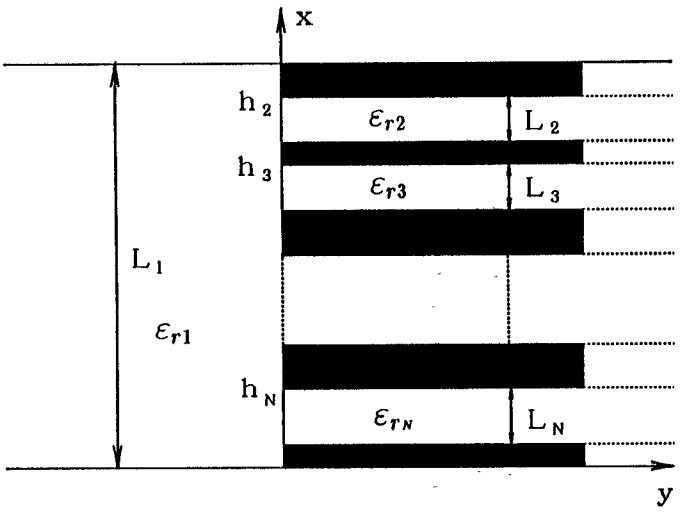

Fig. 2. N-furcated waveguide junction.

as a superposition of the LSE and LSM modes with respect to the z-direction (i.e., the TE and TM modes with respect to the transverse y-direction). Following the conventional transverse resonance procedure [8]–[12], we consider that the LSE and LSM modes propagate in the transverse direction and couple each other at discontinuities of various vertical planes. The hybrid modes as waveguide fields are formed as a result of repeated reflections of the LSE and LSM mode waves at the two ends and discontinuities. Thus, at first we derive the scattering matrix of the N-furcated waveguide junction, as shown in Fig. 2, for the LSE and LSM mode excitation, then we use the generalized scattering matrix technique to obtain the overall transverse scattering matrix of the cascaded discontinuities, and finally we formulate the eigenvalue equation for the propagation constant by using the transverse resonance condition.

A. Treatment of the N-Furcated Waveguide Junction

The hybrid mode fields, $\boldsymbol{E}$ and $\boldsymbol{H}$, are derived from the electric- and magnetic-type Hertzian potential functions, $\boldsymbol{\Pi}^e$ and $\boldsymbol{\Pi}^h$, as follows:

$$\boldsymbol{E} = \nabla \times \nabla \times \boldsymbol{\Pi}^e - j\omega\mu\nabla \times \boldsymbol{\Pi}^h \tag{1}$$

$$\boldsymbol{H} = \nabla \times \nabla \times \boldsymbol{\Pi}^h + j\omega\epsilon\nabla \times \boldsymbol{\Pi}^e. \tag{2}$$

Appropriate solutions for $\boldsymbol{\Pi}^h$ and $\boldsymbol{\Pi}^e$ in the ith waveguide are derived by using the method of the separation of variables and are given by

$$\boldsymbol{\Pi}^h_{in} = \frac{C^h_{in}}{j\sqrt{\omega\mu k^h_{yin}}} \cos k^h_{xin}(x - h_i)e^{-jk^h_{yin}y}e^{-jk_z z}\boldsymbol{i}_y \tag{3}$$

$$\boldsymbol{\Pi}^e_{in} = \frac{C^e_{in}}{j\sqrt{\omega\epsilon_0\epsilon_{ri}k^e_{yin}}} \sin k^e_{xin}(x - h_i)e^{-jk^e_{yin}y}e^{-jk_z z}\boldsymbol{i}_y \tag{4}$$

and the transverse components (with respect to the y-direction) of the fields are then expressed as

$$\boldsymbol{e}^h_{in} = \sqrt{Z^h_{in}}C^h_{in}(-jk_z \cos k^h_{xin}(x - h_i)\boldsymbol{i}_x + k^h_{xin} \sin k^h_{xin}(x - h_i)\boldsymbol{i}_z)e^{-jk_z z} \tag{5a}$$

$$\boldsymbol{h}^h_{in} = \sqrt{Y^h_{in}}C^h_{in}(k^h_{xin} \sin k^h_{xin}(x - h_i)\boldsymbol{i}_x + jk_z \cos k^h_{xin}(x - h_i)\boldsymbol{i}_z)e^{-jk_z z} \tag{5b}$$

$$\boldsymbol{e}^e_{in} = \sqrt{Z^e_{in}}C^e_{in}(-k^e_{xin} \cos k^e_{xin}(x - h_i)\boldsymbol{i}_x + jk_z \sin k^e_{xin}(x - h_i)\boldsymbol{i}_z)e^{-jk_z z} \tag{5c}$$

$$\boldsymbol{h}^e_{in} = \sqrt{Y^e_{in}}C^e_{in}(jk_z \sin k^e_{xin}(x - h_i)\boldsymbol{i}_x + k^e_{xin} \cos k^e_{xin}(x - h_i)\boldsymbol{i}_z)e^{-jk_z z} \tag{5d}$$

where the y-direction propagation constants $k^{h,e}_{yin}$, the wave impedances $Z^{h,e}_{in}$, and the normalization constants $C^{h,e}_{in}$ are defined by

$$k^{h,e}_{xin} = \frac{n\pi}{L_i}$$

$$(k^{h,e}_{cin})^2 = (k^{h,e}_{xin})^2 + (k_z)^2$$

$$(k^{h,e}_{yin})^2 = \omega^2\mu\epsilon_0\epsilon_{ri} - (k^{h,e}_{cin})^2$$

$$Z^h_{in} = \frac{1}{Y^h_{in}} = \frac{\omega\mu}{k^h_{yin}}$$

$$Z^e_{in} = \frac{1}{Y^3_{in}} = \frac{k^e_{yin}}{\omega\epsilon_0\epsilon_{ri}}$$

$$C^h_{in} = \sqrt{\frac{2}{1+\delta_{on}}}\frac{1}{k^h_{cin}\sqrt{L_i}}$$

$$C^e_{in} = \frac{\sqrt{2}}{k^e_{cin}\sqrt{L_i}}$$

$$\delta = \begin{cases} 1, & \text{if } n = 0 \\ 0, & \text{if } n \neq 0 \end{cases}$$

$$n = \begin{cases} 0, 1, 2, \cdots, & \text{for LSE mode} \\ 1, 2, 3, \cdots, & \text{for LSM mode.} \end{cases}$$

If the vector-mode functions, $\tilde{\boldsymbol{e}}_{in}$ and $\tilde{\boldsymbol{h}}_{in}$, are defined by replacing k_z with $-k_z$ in (5a)–(5d) [14], the following orthonormality relations are satisfied:

$$\int_{h_i - L_i}^{h_i} \boldsymbol{e}^h_{in} \times \tilde{\boldsymbol{h}}^h_{im} \cdot \boldsymbol{i}_y\, dx = \int_{h_i - L_i}^{h_i} \tilde{\boldsymbol{e}}^h_{in} \times \boldsymbol{h}^h_{im} \cdot \boldsymbol{i}_y\, dy = \delta_{nm} \tag{6a}$$

$$\int_{h_i - L_i}^{h_i} \boldsymbol{e}^e_{in} \times \tilde{\boldsymbol{h}}^e_{im} \cdot \boldsymbol{i}_y\, dx = \int_{h_i - L_i}^{h_i} \tilde{\boldsymbol{e}}^e_{in} \times \boldsymbol{h}^e_{im} \cdot \boldsymbol{i}_y\, dx = \delta_{nm} \tag{6b}$$

$$\int_{h_i - L_i}^{h_i} \boldsymbol{e}^h_{in} \times \tilde{\boldsymbol{h}}^e_{im} \cdot \boldsymbol{i}_y\, dx = \int_{h_i - L_i}^{h_i} \tilde{\boldsymbol{e}}^h_{in} \times \boldsymbol{h}^e_{im} \cdot \boldsymbol{i}_y\, dx = 0 \tag{6c}$$

$$\int_{h_i - L_i}^{h_i} \boldsymbol{e}^e_{in} \times \tilde{\boldsymbol{h}}^h_{im} \cdot \boldsymbol{i}_y\, dx = \int_{h_i - L_i}^{h_i} \tilde{\boldsymbol{e}}^e_{in} \times \boldsymbol{h}^h_{im} \cdot \boldsymbol{i}_y\, dx = 0 \tag{6d}$$

where δ_{nm} is the Kronecker delta (= 1 if $n = m$; = 0 if $n \neq m$). In the lossless case, k_z is purely real for

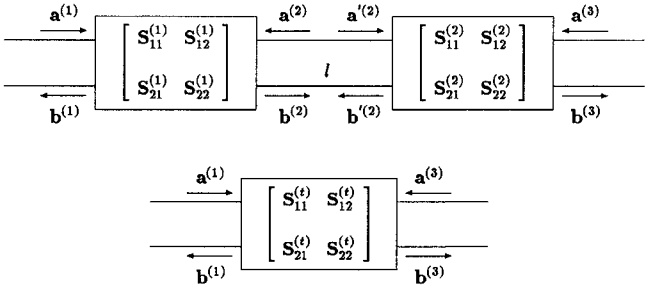

Fig. 3. Scattering matrix representation of cascaded discontinuities.

propagating modes. According to the definition of the tilded-mode functions and to (5), it is evident that when no loss is present the tilded-mode functions are the complex conjugates of those in (5).

Now the electric and magnetic fields in the ith guide at $z = 0$ may be expanded in an infinite sum of LSE- and LSM-mode components as

$$\boldsymbol{E}_{it}(x,y) = \sum_{n=0,1,2,\cdots} (A_{in}^h e^{-jk_{yin}^h y} + B_{in}^h e^{jk_{yin}^h y})\boldsymbol{e}_{in}^h(x) + \sum_{n=1,2,3,\cdots} (A_{in}^e e^{-jk_{yin}^e y} + B_{in}^e e^{jk_{yin}^e y})\boldsymbol{e}_{in}^e(x) \tag{7}$$

$$\boldsymbol{H}_{it}(x,y) = \sum_{n=0,1,2,\cdots} (A_{in}^h e^{-jk_{yin}^h y} - B_{in}^h e^{jk_{yin}^h y})\boldsymbol{h}_{in}^h(x) + \sum_{n=1,2,3,\cdots} (A_{in}^e e^{-jk_{yin}^e y} - B_{in}^e e^{jk_{yin}^e y})\boldsymbol{h}_{in}^e(x) \tag{8}$$

where the coefficients, A_{in} and B_{in}, represent the amplitudes of the incident and reflected (with respect to the y-direction) waves in the ith guide. Using the boundary conditions at $y = 0$ and $z = 0$ and matching the tangential fields, $\boldsymbol{E}_{it}$ and $\boldsymbol{H}_{it}$, lead to a pair of equations on the tangential components of electromagnetic fields. Vector-multiplying the electric component vector equation successively by $\tilde{\boldsymbol{h}}_{1m}^h$ and $\tilde{\boldsymbol{h}}_{1m}^e$, and the magnetic component vector equation successively by $\tilde{\boldsymbol{e}}_{im}^h$ and $\tilde{\boldsymbol{e}}_{im}^e$, using the orthonormality relation (6) and taking truncation on both sides of these equations, we get a set of linear simultaneous equations in the following matrix form:

$$\begin{bmatrix} \mathbf{A}_1^h + \mathbf{B}_1^h \\ \mathbf{A}_1^e + \mathbf{B}_1^e \end{bmatrix} = \begin{bmatrix} \mathbf{R}_{12}^{hh} & \mathbf{R}_{12}^{he} & \cdots & \mathbf{R}_{1N}^{hh} & \mathbf{R}_{1N}^{he} \\ \mathbf{R}_{12}^{eh} & \mathbf{R}_{12}^{ee} & \cdots & \mathbf{R}_{1N}^{eh} & \mathbf{R}_{1N}^{ee} \end{bmatrix} \cdot \begin{bmatrix} \mathbf{A}_2^h + \mathbf{B}_2^h \\ \mathbf{A}_2^e + \mathbf{B}_2^e \\ \vdots \\ \mathbf{A}_N^h + \mathbf{B}_N^h \\ \mathbf{A}_N^e + \mathbf{B}_N^e \end{bmatrix} = [\mathbf{R}] \begin{bmatrix} \mathbf{A}_2^h + \mathbf{B}_2^h \\ \mathbf{A}_2^e + \mathbf{B}_2^e \\ \vdots \\ \mathbf{A}_N^h + \mathbf{B}_N^h \\ \mathbf{A}_N^e + \mathbf{B}_N^e \end{bmatrix} \tag{9}$$

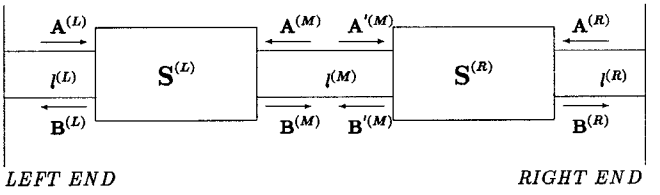

Fig. 4. Application of transverse resonance condition.

$$\begin{bmatrix} \mathbf{B}_2^h - \mathbf{A}_2^h \\ \mathbf{B}_2^e - \mathbf{A}_2^e \\ \vdots \\ \mathbf{B}_N^h - \mathbf{A}_N^h \\ \mathbf{B}_N^e - \mathbf{A}_N^e \end{bmatrix} = \begin{bmatrix} \mathbf{H}_{12}^{hh} & \mathbf{H}_{12}^{eh} \\ \mathbf{H}_{12}^{he} & \mathbf{H}_{12}^{ee} \\ \vdots & \vdots \\ \mathbf{H}_{1N}^{hh} & \mathbf{H}_{1N}^{eh} \\ \mathbf{H}_{1N}^{he} & \mathbf{H}_{1N}^{ee} \end{bmatrix} \begin{bmatrix} \mathbf{A}_1^h - \mathbf{B}_1^h \\ \mathbf{A}_1^e - \mathbf{B}_1^e \end{bmatrix} = [\mathbf{H}] \begin{bmatrix} \mathbf{A}_1^h - \mathbf{B}_1^h \\ \mathbf{A}_1^e - \mathbf{B}_1^e \end{bmatrix} \tag{10}$$

where

$$(\mathbf{R}_{1i}^{hh})_{mn} = \int_{h_i - L_i}^{h_i} \boldsymbol{e}_{in}^h \times \tilde{\boldsymbol{h}}_{1m}^h \cdot \boldsymbol{i}_y \, dx$$

$$(\mathbf{R}_{1i}^{he})_{mn} = \int_{h_i - L_i}^{h_i} \boldsymbol{e}_{in}^e \times \tilde{\boldsymbol{h}}_{1m}^h \cdot \boldsymbol{i}_y \, dx$$

$$(\mathbf{R}_{1i}^{eh})_{mn} = \int_{h_i - L_i}^{h_i} \boldsymbol{e}_{in}^h \times \tilde{\boldsymbol{h}}_{1m}^e \cdot \boldsymbol{i}_y \, dx$$

$$(\mathbf{R}_{1i}^{ee})_{mn} = \int_{h_i - L_i}^{h_i} \boldsymbol{e}_{in}^e \times \tilde{\boldsymbol{h}}_{1m}^e \cdot \boldsymbol{i}_y \, dx$$

$$(\mathbf{H}_{1i}^{hh})_{mn} = \int_{h_i - L_i}^{h_i} \tilde{\boldsymbol{e}}_{im}^h \times \boldsymbol{h}_{1n}^h \cdot \boldsymbol{i}_y \, dx = (\mathbf{R}_{1i}^{hh})_{nm}$$

$$(\mathbf{H}_{1i}^{he})_{mn} = \int_{h_i - L_i}^{h_i} \tilde{\boldsymbol{e}}_{im}^e \times \boldsymbol{h}_{1n}^h \cdot \boldsymbol{i}_y \, dx = (\tilde{\mathbf{R}}_{1i}^{he})_{nm}$$

$$(\mathbf{H}_{1i}^{eh})_{mn} = \int_{h_i - L_i}^{h_i} \tilde{\boldsymbol{e}}_{im}^h \times \boldsymbol{h}_{1n}^e \cdot \boldsymbol{i}_y \, dx = (\tilde{\mathbf{R}}_{1i}^{eh})_{nm}$$

$$(\mathbf{H}_{1i}^{ee})_{mn} = \int_{h_i - L_i}^{h_i} \tilde{\boldsymbol{e}}_{im}^e \times \boldsymbol{h}_{1n}^e \cdot \boldsymbol{i}_y \, dx = (\mathbf{R}_{1i}^{ee})_{nm}$$

where $i = 2, 3, \cdots, N$.

It is emphasized here that the *italic* characters denote space vectors and the Roman characters denote matrices and column vectors. As all the space vector mode-functions in the above integrals are the combinations of sine and cosine functions, the integrations can be analytically carried out easily. The tilded functions $(\tilde{\mathbf{R}}_{1i}^{he})_{nm}$ and $(\tilde{\mathbf{R}}_{1i}^{eh})_{nm}$ are also defined by replacing k_z with $-k_z$ in $(\mathbf{R}_{1i}^{he})_{nm}$ and $(\mathbf{R}_{1i}^{eh})_{nm}$, respectively. From (9) and (10), it is not difficult to deduce the scattering matrix $\mathbf{S}$ of the N-furcated junction in a form as shown below:

$$\begin{bmatrix} \mathbf{B}_1^h \\ \mathbf{B}_1^e \\ \vdots \\ \mathbf{B}_N^h \\ \mathbf{B}_N^e \end{bmatrix} = \begin{bmatrix} \mathbf{S}_{11} & \mathbf{S}_{12} \\ \mathbf{S}_{21} & \mathbf{S}_{22} \end{bmatrix} \begin{bmatrix} \boldsymbol{A}_1^h \\ \boldsymbol{A}_1^e \\ \vdots \\ \boldsymbol{A}_N^h \\ \boldsymbol{A}_N^e \end{bmatrix} \tag{11}$$

where

$$\mathbf{S}_{22} = (\mathbf{I} + \mathbf{HR})^{-1}(\mathbf{I} - \mathbf{HR}) = 2(\mathbf{I} + \mathbf{HR})^{-1} - \mathbf{I} \tag{12a}$$

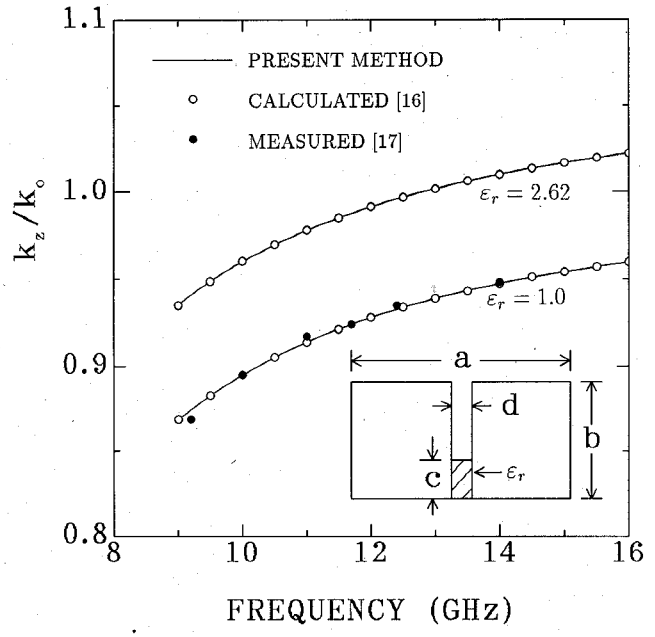

Fig. 5. Normalized propagation constant versus frequency for dielectric-loaded single-ridged waveguides; $a = 19$ mm, $b = 9.5$ mm, $c = 1.7$ mm, $d = 0.3$ mm.

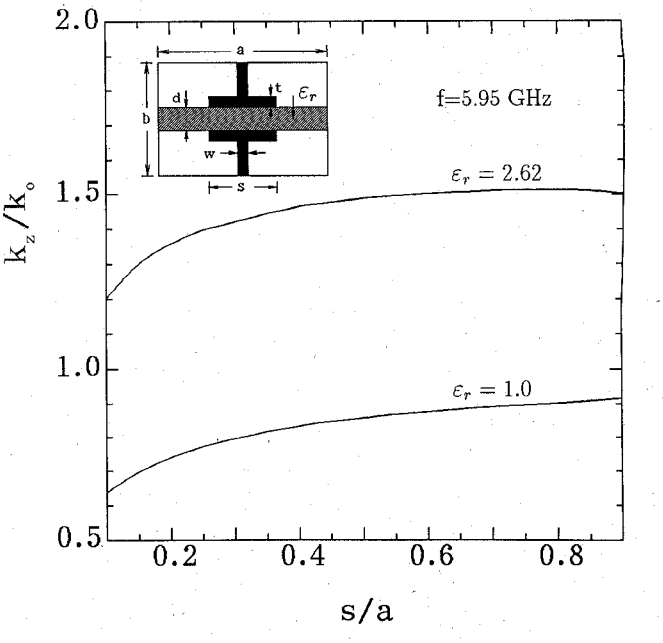

Fig. 7. Normalized propagation constant as a function of septum width s for the first TE mode of dielectric-loaded T-septum waveguides: $b/a = 0.5, w/a = 0.1, d/b = 0.2, t/b = 0.05$.

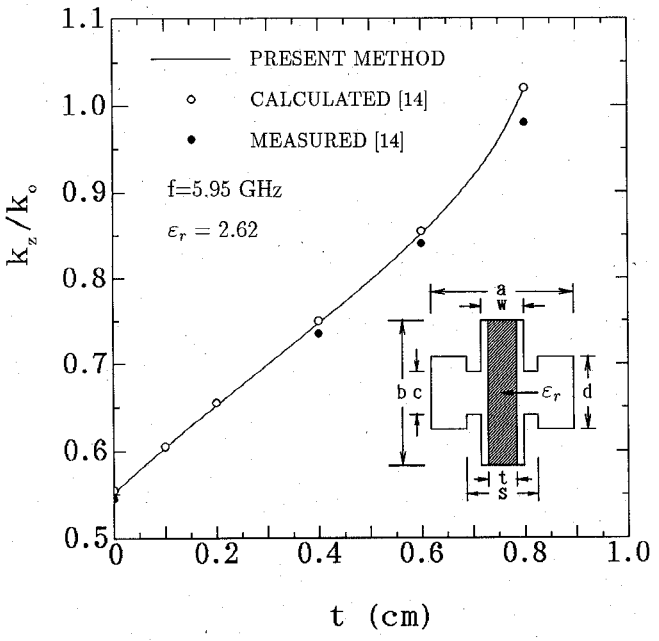

Fig. 6. Normalized propagation constant versus dielectric slab thickness t for a slotted dielectric-loaded ridge waveguide; $a = 26.264$ mm, $b = 26.882$ mm, $c = 6.502$ mm, $d = 11.760$ mm, $w = 8.026$ mm, $s = 13.081$ mm.

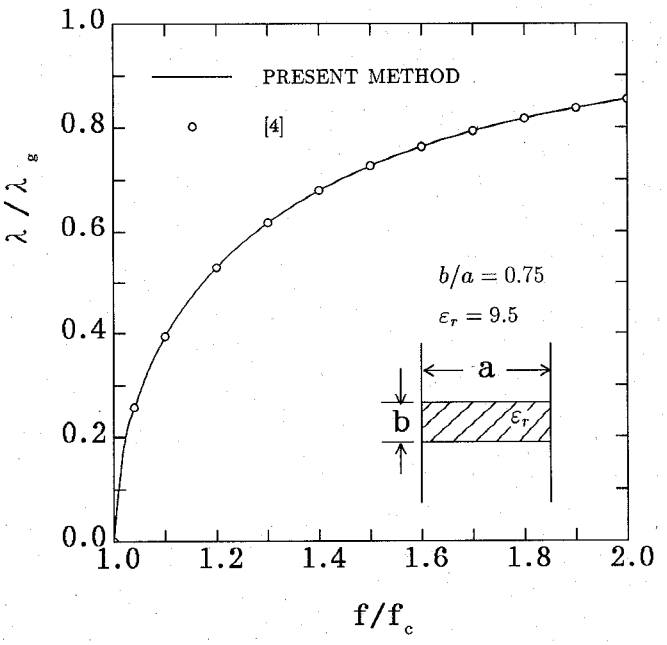

Fig. 8. Dispersion curve of a nonradiative alumina waveguide.

$$\mathbf{S}_{21} = 2(\mathbf{I} + \mathbf{HR})^{-1}\mathbf{H} = (\mathbf{S}_{22} + \mathbf{I})\mathbf{H} \tag{12b}$$

$$\mathbf{S}_{12} = 2\mathbf{R}(\mathbf{I} + \mathbf{HR})^{-1} = \mathbf{R}(\mathbf{S}_{22} + \mathbf{I}) \tag{12c}$$

$$\mathbf{S}_{11} = \mathbf{S}_{12}\mathbf{H} - \mathbf{I} = \mathbf{R}\mathbf{S}_{21} - \mathbf{I}. \tag{12d}$$

B. Cascaded Discontinuities

In the case of cascaded discontinuities, there are two approaches. The first is to combine the transmission matrices of individual discontinuities for expressing the overall transmission matrix, and it requires an equal number of modes in any of the sections connecting discontinuities. As is well known, however, the mode-matching analysis usually requires a proper choice of the number of modal terms retained in the guides connected to the junction to overcome the relative convergence problem [10]–[12], and it has been shown in [10] that the requirement of an equal number of modal terms in any of the sections may violate the edge condition, resulting in incorrect numerical solutions. Thus, in this paper, the cascaded discon-

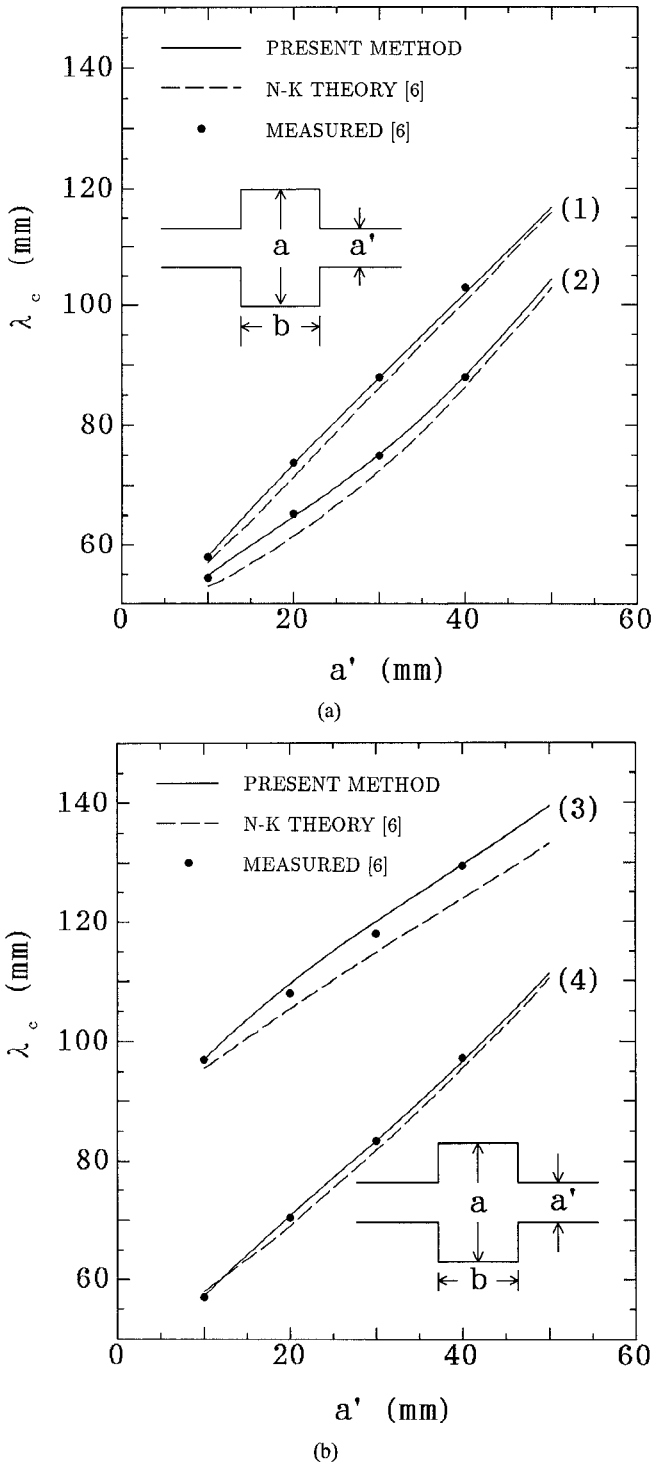

Fig. 9. Comparison between measured and theoretical values of the cutoff wavelength λ_c for groove guides of various cross sections. (a) Curves (1) and (2), where (1) $a = a' + 20$ mm, $b = 30$ mm, (2) $a = a' + 20$ mm, $b = 10$ mm. (b) Curves (3) and (4), where (3) $a = a' + 40$ mm, $b = 20$ mm, (4) $a = a' + 20$ mm, $b = 20$ mm.

tinuity problems are treated by using the second approach, i.e., the generalized scattering matrix method [12].

Referring to Fig. 3, the submatrices of the overall scattering matrix (superscript t) of two cascaded junctions, separated by a uniform line section of length l, are given by

$$\mathbf{S}_{11}^{(t)} = \mathbf{S}_{11}^{(1)} + \mathbf{S}_{12}^{(1)}\mathbf{E}\mathbf{D}\mathbf{S}_{11}^{(2)}\mathbf{D}\mathbf{S}_{21}^{(1)} \tag{13a}$$

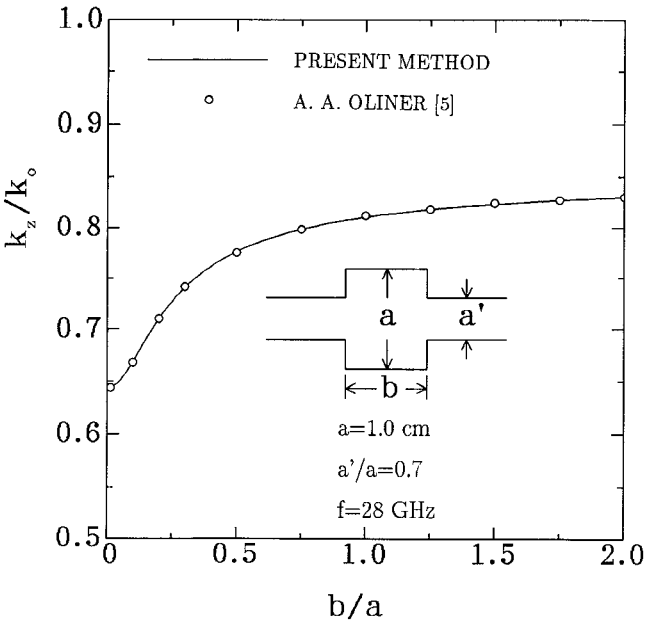

Fig. 10. Variation of propagation constant versus groove guide aspect ratio b/a.

$$\mathbf{S}_{12}^{(t)} = \mathbf{S}_{12}^{(1)}\mathbf{E}\mathbf{D}\mathbf{S}_{12}^{(2)} \tag{13b}$$

$$\mathbf{S}_{21}^{(t)} = \mathbf{S}_{21}^{(2)}\mathbf{D}\mathbf{F}\mathbf{S}_{21}^{(1)} \tag{13c}$$

$$\mathbf{S}_{22}^{(t)} = \mathbf{S}_{22}^{(2)} + \mathbf{S}_{21}^{(2)}\mathbf{D}\mathbf{F}\mathbf{S}_{22}^{(1)}\mathbf{D}\mathbf{S}_{12}^{(2)} \tag{13d}$$

where

$$\mathbf{E} = (\mathbf{I} - \mathbf{D}\mathbf{S}_{11}^{(2)}\mathbf{D}\mathbf{S}_{22}^{(1)}\mathbf{D})^{-1}$$

$$\mathbf{F} = (\mathbf{I} - \mathbf{S}_{22}^{(1)}\mathbf{D}\mathbf{S}_{11}^{(2)}\mathbf{D})^{-1}$$

$$\mathbf{D} = \begin{bmatrix} \mathbf{D}^h & \mathbf{0} \\ \mathbf{0} & \mathbf{D}^e \end{bmatrix} \tag{14}$$

and $\mathbf{D}^h$ and $\mathbf{D}^e$ are diagonal matrices whose diagonal elements are given by

$$\mathrm{D}_{nn}^h = e^{-jk_{y_{nn}}^h l}; \quad \mathrm{D}_{nn}^e = e^{-jk_{y_{nn}}^e l}. \tag{15}$$

C. Transverse Resonance Condition and Eigenvalue Equation

Out of the uniform sections connecting the discontinuities, we choose one having the smallest vertical dimension (with respect to the transverse resonance y-direction, i.e., the horizontal direction), and use $\mathbf{S}^{(L)}$ and $\mathbf{S}^{(R)}$ to indicate the overall scattering matrices of the cascaded discontinuities on its left and right side, respectively, as indicated in Fig. 4. The column vectors, $\mathbf{A}^{(L)}$ and $\mathbf{B}^{(L)}$, counting for incident and reflected wave amplitudes, respectively, of matrix $\mathbf{S}^{(L)}$ in the left end region, and vectors $\mathbf{A}^{(R)}$ and $\mathbf{B}^{(R)}$ of matrix $\mathbf{S}^{(R)}$ in the right end region, are related through the two end boundaries, which may be an electric wall (short-circuited) or a magnetic wall (open-circuited), as follows:

$$\mathbf{A}^{(L)} = \mp\mathbf{D}^{(L)}\mathbf{D}^{(L)}\mathbf{B}^{(L)};$$

$$\mathbf{A}^{(R)} = \mp\mathbf{D}^{(R)}\mathbf{D}^{(R)}\mathbf{B}^{(R)} \tag{16}$$

where the sign $\mp$ corresponds to the electric (upper one) and magnetic (lower one) wall, respectively. In the middle section,

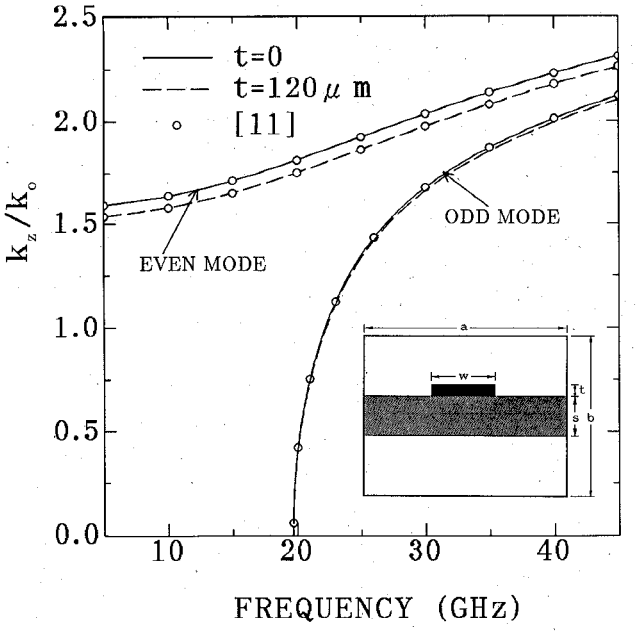

Fig. 11. Normalized propagation constant as a function of frequency for a suspended microstrip lines. $a = 2b = 7.112$ mm, $s = 0.635$ mm, $w = 1.0$ mm, $\epsilon_r = 9.6$.

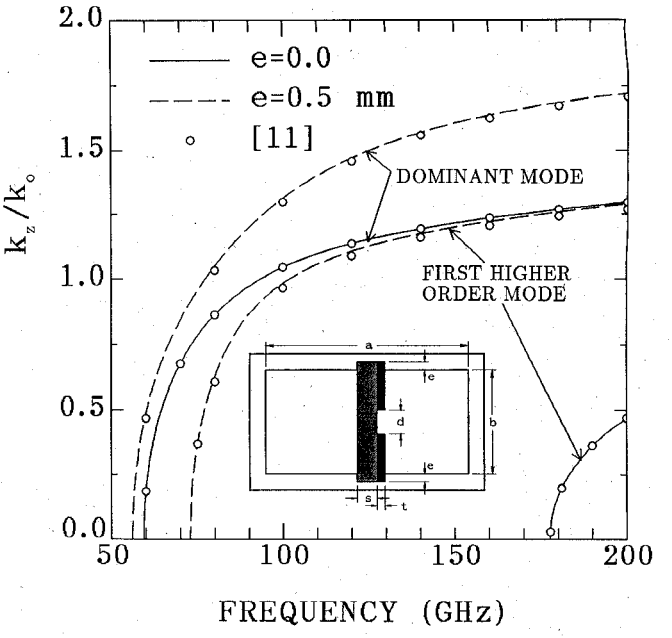

Fig. 12. Propagation characteristics of the dominant and the first higher odd mode in a unilateral finline with mounting grooves. $a = 2b = 1.65$ mm, $s = 0.11$ mm, $d = 0.3$ mm, $t = 5\,\mu$m, $\epsilon_r = 3.75$.

the forward and backward wave amplitudes are related by

$$\mathbf{A}^{(M)} = \mathbf{D}^{(M)}\mathbf{B}'^{(M)}; \quad \mathbf{A}'^{(M)} = \mathbf{D}^{(M)}\mathbf{B}^{(M)} \tag{17}$$

where $\mathbf{A}^{(M)}$ and $\mathbf{B}^{(M)}$ are the amplitude column vectors of the incident and reflected modes, respectively, of matrix $\mathbf{S}^{(L)}$ in the middle section, and $\mathbf{A}'^{(M)}$ and $\mathbf{B}'^{(M)}$ of matrix $\mathbf{S}^{(R)}$. The diagonal elements in the diagonal matrices, $\mathbf{D}^{(L)}, \mathbf{D}^{(R)}$ and $\mathbf{D}^{(M)}$, are defined in a similar way to that of (14) and (15), with the transverse propagation constant and propagation length l of the corresponding section.

Substituting (16) and (17) into the scattering matrix expressions of $\mathbf{S}^{(L)}$ and $\mathbf{S}^{(R)}$, the amplitude column vectors, $\mathbf{A}^{(L)}, \mathbf{B}^{(L)}, \mathbf{A}^{(R)}, \mathbf{B}^{(R)}, \mathbf{A}^{(M)}$, and $\mathbf{A}'^{(M)}$, may be eliminated, and $\mathbf{B}^{(M)}$ and $\mathbf{B}'^{(M)}$ are related by

$$\mathbf{B}^{(M)} = (\mathbf{S}_{21}^{(L)}\mathbf{E}^{(L)}\mathbf{S}_{12}^{(L)} + \mathbf{S}_{22}^{(L)})\mathbf{D}^{(M)}\mathbf{B}'^{(M)} \tag{18}$$

$$\mathbf{B}'^{(M)} = (\mathbf{S}_{21}^{(R)}\mathbf{E}^{(R)}\mathbf{S}_{12}^{(R)} + \mathbf{S}_{22}^{(R)})\mathbf{D}^{(M)}\mathbf{B}^{(M)} \tag{19}$$

where $\mathbf{E}^{(L)}$ and $\mathbf{E}^{(R)}$ are defined as

$$\mathbf{E}^{(L)} = \mathbf{D}^{(L)}\mathbf{D}^{(L)}(\mathbf{I} - \mathbf{S}_{11}^{(L)}\mathbf{D}^{(L)}\mathbf{D}^{(L)})^{-1}$$

$$\mathbf{E}^{(R)} = \mathbf{D}^{(R)}\mathbf{D}^{(R)}(\mathbf{I} - \mathbf{S}_{11}^{(R)}\mathbf{D}^{(R)}\mathbf{D}^{(R)})^{-1}.$$

For the existence of nontrivial solutions for the linear simultaneous equations, (18) and (19), the determinant should vanish, that is, the following eigenvalue equation should be solved:

$$\det \mathbf{G} = 0 \tag{20}$$

where

$$\mathbf{G} = \mathbf{I} - (\mathbf{S}_{21}^{(L)}\mathbf{E}^{(L)}\mathbf{S}_{12}^{(L)} + \mathbf{S}_{22}^{(L)})\mathbf{D}^{(M)} \cdot (\mathbf{S}_{21}^{(R)}\mathbf{E}^{(R)}\mathbf{S}_{12}^{(R)} + \mathbf{S}_{22}^{(R)})\mathbf{D}^{(M)}. \tag{21}$$

For open structures, like the NRD waveguide and the groove guide, the left and right end extend to infinity, so that there will be no reflections from the two ends. In such cases, the matrices, $\mathbf{D}^{(L)}$ and $\mathbf{D}^{(R)}$, representing wave reflections at the two end boundaries become *zero matrices,* and the final eigenvalue matrix $\mathbf{G}$ in (21) is much simplified to

$$\mathbf{G} = \mathbf{I} - \mathbf{S}_{22}^{(L)}\mathbf{D}^{(M)}\mathbf{S}_{22}^{(R)}\mathbf{D}^{(M)}. \tag{22}$$

With such a treatment of the open ends, we succeed in avoiding the usual assumption of placing perfect conduct planes on the two far sides of the guide, as pointed out in the introduction.

By using the transverse resonance condition at the section with the smallest vertical dimension, we obtain the final eigenvalue matrix $\mathbf{G}$ with the smallest size as the number of modal terms is the smallest in this region.

The commonly used transverse resonance procedure in other papers [8], [9], on the contrary, is to treat the cascaded discontinuities from the left to the right or from the right to the left in sequence, and then to impose the two end boundary conditons. This procedure usually results in a large eigenvalue matrix since the two end sections are large in dimensions in most practical configurations.

Moreover, we may notice that as the coefficients of the mode functions in (5) are normalized, the elements in the scattering matrices, $\mathbf{S}^{(L)}$ and $\mathbf{S}^{(R)}$, are of order 1; and that the elements in the diagonal matrices $\mathbf{D}^{(L)}$, $\mathbf{D}^{(M)}$, $\mathbf{D}^{(R)}$ exponentially decay (in the y-direction) for higher evanescent modes, so that the eigenvalue matrix $\mathbf{G}$ in (21) or (22) is diagonal dominant with the diagonal elements of order 1. The reduced size of the eigenvalue matrix and the good property of the matrix elements enable the numerical computation process to be quite stable with the determinant of the eigenvalue matrix neither too large nor too small, thus greatly easing the root searching process for eigenvalues. This is another merit of our method against the conventionally used transverse resonance treatment and is also one of the main different points from the theory of

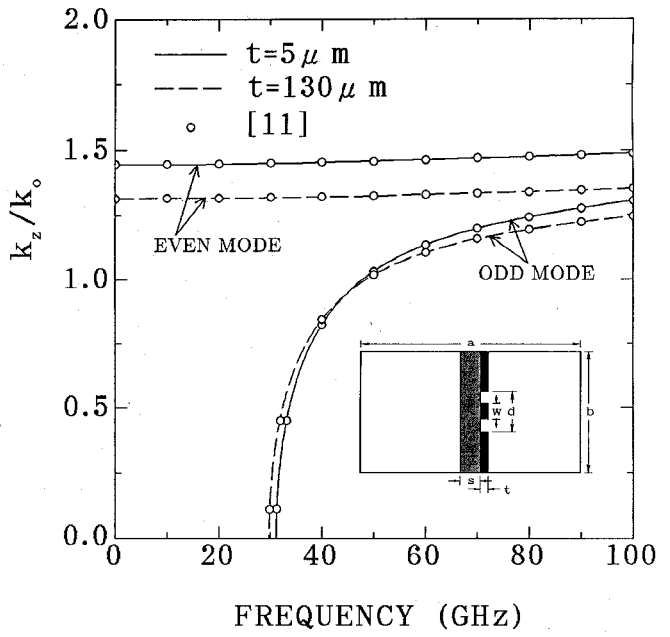

Fig. 13. Normalized propagation constant versus frequency in coplanar waveguide. $a = 2b = 3.1$ mm, $s = 0.22$ mm, $d = 0.6$ mm, $w = 0.2$ mm, $\epsilon_r = 3.75$.

a recent paper [19] which took a similar analysis process for the characterization of MMIC transmission lines. Usually after several searching steps, the root of (20) may rapidly converge to results with good accuracy in the present method.

III. Numerical Examples and Discussions

The above stated process has been programmed for numerical calculation. As an illustration of the versatility and validity of this method, results on the dispersion characteristics of some waveguiding structures are provided, and comparisons with previous techniques are made.

A. Ridged Waveguide and Its Variations

Ridged waveguide has been on stage for a long years [13], but is still receiving attentions up to now, and many of its variations, such as slotted, dielectric loaded ridged waveguides and T-septum waveguides, have appeared [14]–[16]. Since the first complete spectrum analysis of a ridged waveguide was given by Montgomery [13], who used the Ritz–Galerkin procedure, most of the papers on ridged waveguides and its variations published since then [14], [15] followed the same approach. In their analysis, all of the unknown expansion modal coefficients of fields remained in the final eigenvalue matrix, so that the size of the matrix was large which might cause difficulty in computation. When the number of subregions increases, this problem becomes even more serious. A recent paper [16] has used a mixed spectral-domain method to treat ridged waveguide problems, and it is more flexible and more numerically efficient than the previous methods. However, it is actually complicated in mathematical formulations because of the complicated configurations of the ridged waveguides with multisubregions. Our theory stated in Section II is simpler and more versatile.

The frequency dependence of the propagation constant of a single-ridged waveguide is shown in Fig. 5 which is about the same for the two dielectric slab loading. As can be seen, our results agree very well with both calculated results [16] by the mixed spectral-domain method and the experiment data [17].

Figure 6 shows the dependence of the propagation constant on the dielectric slab thickness t, and it reveals a marked increase in cutoff wavelength when the dielectric slab thickness increases. Such a dependence can also be observed in Fig. 7, which shows the propagation constants as a function of the septum width s of a T-septum waveguide with and without dielectric loading.

For the correct convergence of the numerical results by the mode-matching method, it is well known that the modes in every subregions should be retained according to the ratios between the sub-region heights. Taking the structure shown in Fig. 6 as an example, the mode ratio is approximately taken according to the ratio $b : c : d$, and we found that 3 LSE and LSM modes in the region of height c, 6 of height d and 15 of height b, respectively, are adequate for obtaining converged results.

B. NRD Waveguide and Groove Guide

The NRD waveguide and groove guide are two of several low-loss waveguides proposed for use at millimeter wavelengths [4]–[6]. In Fig. 8, the dispersion curve of a nonradiative alumina waveguide is illustrated, where the solid line indicates present results, and the dots those of [4] based on the formulation of the H-guide theory [18]. In Fig. 9, comparisons between measured and theoretical values of the cutoff wavelength λ_c for groove guides of various cross sections are provided. The solid lines represent our theory, the dashed curves are the first-order approximation theoretical values [6], and the points are the measured results of Nakahara and Kurauchi [6]. Figure 10 indicates variation of propagation constant with groove guide aspect ratio b/a, and good agreement has been found between our theory and the results of Oliner and Lampariello [5]. The rule of thumb equivalent network analysis in [5] is simple and very accurate, but is only valid for the dominat mode.

C. Planar Transmission Lines

Among the published rigorous techniques for analyzing planar transmission lines are the spectral-domain technique and the singular integral equation method. Although these techniques have a very good numerical efficiency, they do not include the effects of metallization thickness and substrate mounting grooves. The metallization thickness has been taken into account in [8], [9] using the mode-matching technique, but all requires an equal number of modal terms in the subregions forming the guide. As has been shown in [10], this requirement may violate the edge-condition and may fail to provide accurate results.

Figure 11 shows the effect of the metallization thickness on the propagation constants of the first even and odd mode in the suspended microstrip line. A noticeable effect is only observed on the dominant mode. On the other hand, the effect of the substrate mounting groove on the propagation characteristics is quite significant for both the dominant and the first higher order mode of the unilateral finline, as shown in Fig. 12. As

pointed out by [11], the cutoff frequency of the first higher order mode decreases significantly when the mounting groove is used, leading to a very large reduction in the single-mode bandwidth. Finally, the metallization thickness effect on the propagation constants in coplanar waveguides is illustrated in Fig. 13. While the influence on the odd mode is negligible, it is, however, pronounced on the dominant mode over the whole frequency range. In the above figures, the solid curves are our results, the dots are those of [11], and the agreements are excellent.

IV. Conclusion

A unified transverse scattering matrix approach has been presented to analyze transmission line eigenvalue problems. The formulation allows one to treat a wide variety of waveguiding structures including open structures. Comparisons with previous approaches prove that it is simple, versatile, accurate, and efficient. Application of this method to other eigenvalue problems such as the determination of resonant frequencies of complex cavities is straightforward.

References

[1] T. Itoh, *Numerical Techniques for Microwave and Millimeter-Wave Passive Structures.* New York: Wiley, 1989.

[2] R. Sorrentino, *Numerical Methods for Passive Microwave and Millimeter-Wave Structures.* New York: IEEE Press, 1989.

[3] E. Yamashita, Ed., *Analysis Methods for Electromagnetic Wave Problems.* Boston: Artech House, 1990.

[4] T. Yoneyama and S. Nishida, "Nonradiative dielectric waveguide for millimeter-wave integrated circuits," *IEEE Trans. Microwave Theory Tech.,* vol. MTT-29, pp. 1188–1192, Nov. 1981.

[5] A. A. Oliner and P. Lampariello, "The dominant mode properties of open groove guide: an improved solution," *IEEE Trans. Microwave Theory Tech.,* vol. MTT-33, pp. 755–764, Sep. 1985.

[6] T. Nakahara and N. Kurauchi, "Transmission modes in the grooved guide," *J. Inst. Electron. Commun. Eng. Jap.,* vol. 47, no. 7, pp. 43–51, July 1964.

[7] R. Vahldieck and J. Ruxton, "A broadband groove guide coupler for millimeter-wave applications," in *IEEE MTT-S Int. Microwave Symp. Dig.,* 1987, pp. 349–352.

[8] R. Vahldieck and J. Bornemann, "A modified mode matching technique and its application to a class of quasi-planar transmission lines," *IEEE Trans. Microwave Theory Tech.,* vol. MTT-33, pp. 916–926, Oct. 1985.

[9] J. Bornemann and F. Arndt, "Calculating the characteristic impedance of finlines by the transverse resonance method," *IEEE Trans. Microwave Theory Tech.,* vol. MTT-34, pp. 85–92, Jan. 1986.

[10] R. R. Mansour and R. H. Macphie, "An improved transmission matrix formulation of cascaded discontinuities and its application to E-plane circuits," *IEEE Trans. Microwave Theory Tech.,* vol. MTT-34, pp. 1490–1498, Dec. 1986.

[11] R. R. Mansour and R. H. Macphie, "A unified hybrid-mode analysis for planar transmission lines with multilayer isotropic/anisotropic substrates," *IEEE Trans. Microwave Theory Tech.,* vol. MTT-35, pp. 1382–1391, Dec. 1987.

[12] R. Mittra and S. W. Lee, *Analytical Techniques in the Theory of Guided Waves.* New York: Macmillan, 1971.

[13] J. P. Montgomery, "On the complete eigenvalue solution of ridged waveguide," *IEEE Trans. Microwave Theory Tech.,* vol. MTT-19, pp. 547–555, June 1971.

[14] A. T. Villeneuve, "Analysis of slotted, dielectrically loaded, ridged waveguide," *IEEE Trans. Microwave Theory Tech.,* vol. MTT-32, pp. 1302–1310, Oct. 1984.

[15] G. G. Mazumder and P. K. Saha, "A novel waveguide with double T-septums," *IEEE Trans. Microwave Theory Tech.,* vol. MTT-35, pp. 201–204, Feb. 1987.

[16] K. T. Ng and C. H. Chan, "Unified solution of various dielectric-loaded ridge waveguides with a mixed spectral-domain method," *IEEE Trans. Microwave Theory Tech.,* vol. MTT-37, pp. 2080–2085, Dec. 1989.

[17] Y. Utsumi, "Variational analysis of ridged waveguide modes," *IEEE Trans. Microwave Theory Tech.,* vol. MTT-33, pp. 111–120, Feb. 1985.

[18] F. J. Tischer, "H guide with laminated dielectric slab," *IEEE Trans. Microwave Theory Tech.,* vol. MTT-18, pp. 9–15, Jan. 1970.

[19] J. Bornemann, "A scattering-type transverse resonance technique for the calculation of (M)MIC transmission line characteristics," *IEEE Trans. Microwave Theory Tech.,* vol. MTT-39, pp. 2083–2088, Dec. 1991.

Zhewang Ma was born in Anhui, China, on July 7, 1964. He received the B.E. and M.E. degrees from the University of Science and Technology of China, Hefei, China, in 1986 and 1989, respectively, and is currently working towards the Ph.D. degree in the electronic engineering at the University of Electro-communications, Tokyo, Japan.

He has done research on dielectric waveguides and resonators, millimeter leaky-wave antennas. His present interests are in the analysis and design of microwave and millimeter-wave integrated circuits and antennas.

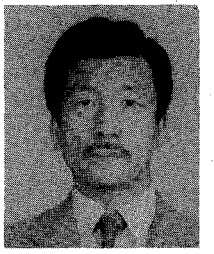

Eikichi Yamashita (F'84) was born in Tokyo, Japan, on February 4, 1933. He received the B.S. degree from the University of Electro-communications, Tokyo, Japan, and the M.S. and Ph.D. degrees from the University of Illinois, Urbana, all in electrical engineering, in 1956, 1963, and 1966, respectively.

From 1956 to 1964, he was a Member of the Research Staff on millimeter-wave engineering at the Electrotechnical Laboratory, Tokyo, Japan. While on leave from 1961 to 1963 and from 1964 to 1966, he studied solid-state devices in the millimeter-wave region at the Electro-Physics Laboratory, University of Illinois. He became Associate Professor in 1967 and Professor in 1977 in the Department of Electronic Engineering, the University Electro-communications, Tokyo, Japan. His research work since 1956 has been principally on applications of electromagnetic waves such as various microstrip transmission lines, wave propagation in gaseous plasma, pyroelectric-effect detectors in the submillimeter-wave region, tunnel-diode oscillators, wide-band laser modulators, various types of optical fibers, and ultra-short electrical pulse propagation on transmission lines.

Dr. Yamashita was Chairperson of the Technical Group on Microwaves, IEICE, Japan, for the period 1985–1986 and Vice-Chairperson, Steering Committee, Electronics Group, IEICE, for the period 1989–1990. He was elected Chairperson of the MTT-S Tokyo Chapter of IEEE for the period 1985–1986. He served as Chairperson of International Steering Committee, 1990 Asia-Pacific Microwave Conference, held in Tokyo.

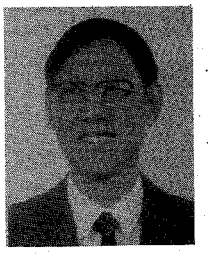

Shanjia Xu (SM'91) graduated from the University of Science and Technology of China in 1965.

Since then, he has been with the same University as a Professor and Associate Chairman of the Department of Radio and Electronics since 1986. From 1983 to 1986 he was a Visiting Scholar at the Polytechnic Institute of New York. During the winter of 1991, he was a Guest Scientist in Wurzburg University Germany. Also, he was an academic visitor at several universities in the United States, Canada, Japan, Germany, and Hong Kong. He has been teaching microwave engineering courses for more than 25 years for graduate and undergraduate students. He has been engaged in research in the fields of microwave and millimeter wave theory and techniques and has been participating in many research programs in cooperation with institutes and industrial laboratories and has received the second and the third award for science and technology advances given by the Chinese Academy of Sciences. He has published over 100 papers in various of academic journals and proceedings of international conferences. His research interests are in the areas of nonuniform dielectric waveguides and applications, numerical techniques in electromagnetics, and millimeter-wave technology.

Mr. Xu is a member of the editoral board of the *Journal of Infrared and Millimeter Waves* and is a standing member of the editoral board of the *Journal of the China Institute of Communications.* He is Associate Chairman of the millimeter and sub-millimeter wave speciality of Chinese MTT Society. His biography was listed in the *Who's Who of the Asian Pacific Rim.*